Journal of Cerebral Blood Flow & Metabolism (2015) 35, 951–958

www.jcbfm.com

ORIGINAL ARTICLE

Ischemic tolerance in pre-myelinated white matter: the role of astrocyte glycogen in brain pathology

Robert Fern

In isolated white matter, ischemic tolerance changes dramatically in the period immediately before the onset of myelination. In the absence of an extrinsic energy source, postnatal day 0 to 2 (P0 to P2) white matter axons are here shown to maintain excitability for over twice as long as axons >P2, a differential that was dependent on glycogen metabolism. Prolonged withdrawal of extrinsic energy supply tended to spare axons in zones around astrocytes, which are shown to be the sole repository for glycogen particles in developing white matter. Analysis of mitochondrial volume fraction revealed that neither axons nor astrocytes had a low metabolic rate in neonatal white matter, while oligodendroglia at older ages had an elevated metabolism. The astrocyte population is established early in neural development, and exhibits reduced cell density as maturation progresses and white matter expands. The findings show that this event establishes the necessary conditions for ischemia sensitivity in white matter and indicates that astrocyte proximity may be significant for the survival of neuronal elements in conditions associated with compromised energy supply.

Journal of Cerebral Blood Flow & Metabolism (2015) **35,** 951–958; doi:10.1038/jcbfm.2015.3; published online 11 February 2015

Keywords: axon; astrocyte; glia; glycogen; ischemia; white matter

INTRODUCTION

Brain ischemia is associated with depletion in the energy and oxygen supply required by all cells to maintain essential functions such as ion homeostasis. In the adult brain, acute ischemia leads to stroke injury while partial ischemia has been linked to a variety of neurological diseases including multiple sclerosis and neurodegeneration.[1] In the developing nervous system, focal and diffuse ischemic injuries to white matter structures are a major cause of developmental neurological pathology with a peak incidence between 20 and 32 post-conception weeks (PCWs).[2,3] In humans, central myelination starts around the time of birth and the white matter affected in these injuries is therefore pre-myelinated. The window of clinical susceptibility spans the period when oligodendrocyte precursor cells mature into highly ischemia-sensitive pre-oligodendrocytes (Pre-Ols)[2] as the tissue prepared for the onset of myelination. Mature-phenotype astrocytes populate the intermediate zone from 16 to 18 PCWs, well before the onset of susceptibility to ischemic injury and before oligodendroglial lineage cells start to mature. The white matter astrocytes are rich in glycogen particles,[4,5] but their significance for injury is unknown.

These observations on human white matter development agree with those from the most fully described white matter animal model, the rat optic nerve (RON). At birth, the RON contains only small diameter pre-myelinated axons, mature-phenotype astrocytes, and a small population of immature glial cells, placing it at a similar developmental point to early human white matter structures. The RON is populated by oligodendrocyte precursor cells from P2 onwards and pre-Ols appear around P5, with myelinating oligodendrocytes present from P7.[6,7] Axon enlargement is first seen between P2 and P7 and the first axo-glial contacts are reported at P6. In the RON, ischemic conditions modeled by oxygen–glucose deprivation (OGD) produce a pattern of injury with very high tolerance between P0 and P2, while the P3 to P10 RON is resistant to glucose withdrawal but not to OGD.[8]

Here, we test various forms of energy deprivation on the ability of the developing RON to maintain action potential conduction and axon structural integrity, focusing on the curious ischemia tolerance present in white matter before the start of axon enlargement (P0 to P2). Several explanations might underlie the high ischemia tolerance of white matter at this point: (1) a low metabolic rate; (2) a high cellular resistance to energy deprivation; or (3) the presence of an oxygen-insensitive energy reserve. The only significant energy reserve in the central nervous system is glycogen, which is largely restricted to astrocytes.[9] There is evidence for an energy shuttle operating between astrocytes and axons in adult white matter, possibly mediated by lactate release and uptake.[10] However, metabolic intermediates such as lactate cannot be used in the absence of oxygen, and the mechanism responsible for the ischemia tolerance of early pre-myelinating white matter is unknown.

MATERIALS AND METHODS

UK home office regulations were followed for all experimental work, which was conducted in accordance with the relevant guidelines and regulations. The animal welfare and ethics committee of the University of Leicester approved all the experimental protocols. Optic nerves were dissected from Lister-hooded rats of both sexes and were perfused with artificial cerebrospinal fluid (aCSF), composition: NaCl 126 mM; KCl 3 mM; NaH_2PO_4 2 mM; $MgSO_4$ 2 mM; $CaCl_2$ 2 mM; $NaHCO_3$ 26 mM; glucose 10 mM; pH 7.45, bubbled with 5% CO_2/95% O_2, and maintained at 37°C. For OGD, aCSF was

Peninsula School of Medicine and Dentistry, University of Plymouth, Plymouth, UK. Correspondence: Professor R Fern, Peninsula School of Medicine and Dentistry, University of Plymouth, John Bull Building, Research Way, Plymouth PL6 8BU, UK.
E-mail: robert.fern@plymouth.ac.uk
Received 20 October 2014; revised 15 December 2014; accepted 17 December 2014; published online 11 February 2015

replaced by glucose-free aCSF saturated with a 95% N_2/5% CO_2 mixture. The chamber atmosphere was switched to 5% CO_2/95% N_2 during OGD perfusion. Osmolarity of solutions was measured and adjusted as required. Data are represented as mean ± s.e.m., significance was determined by *t*-test or analysis of variance as appropriate. Reagents were from Sigma (Gillingham, UK) unless otherwise stated.

Electrophysiology

The electrophysiological recording techniques have been describe previously.[8] In brief, compound action potentials (CAPs) were evoked and recorded with glass electrodes, and peak-to-peak amplitude was used to assess changes in excitability. Compound action potentials were evoked via square-wave constant current pulses (Iso stim A320, WPI), amplified (Cyber Amp 320, Axon Instruments, Sunnyvale, CA, USA), subtracted from a parallel differential electrode, filtered (low pass: 800–10,000 Hz), digitized (1401 mini, Cambridge Electronic Design, Cambridge, UK), and displayed on a PC running Signal software (Cambridge Electronic Design). Non-recoverable CAP loss from the optic nerve indicates irreversible failure of axon function.[11]

Electron Microscopy

RONs were washed in Sorenson's buffer and post-fixed in 3% gluteraldehyde/Sorenson's. Nerves were fixed (2% osmium tetroxide) and dehydrated before epoxy infiltration. Ultrathin sections were counter-stained with uranyl acetate, lead citrate, and 1% osmium tetroxide/1.5% potassium ferricyanide before examination with a Jeol (Welwyn Garden City, UK) 100CX electron microscope. For morphometric analysis and viability scoring, axons within a minimum of three grid sections were outlined by hand (Image-J software, NIH, Bethesda, MD, USA), and the axon area and perimeter were measured. Axon diameter was taken as the mean of the longest and shortest widths. Grids were randomly selected and all identifiable axons within the area were included. Axon viability was determined using the following criteria (see ref. 11): (i) the presence of an intact axolemma; (ii) the presence of microtubules; and (iii) the presence of a debris-free axoplasm. Axons that showed two or more of these attributes were considered viable.

RESULTS

The metabolic pathways for energy utilization in white matter include a glycogen energy reserve located in astrocytes and an energy shuttle between astrocytes and axons probably mediated by lactate. After the withdrawal of glucose, glycogen and metabolic intermediates will continue to fuel metabolism and maintain energy-dependent ion homeostasis via transport proteins such as the Na-K ATPase. The extent to which this can maintain excitability in developing axons is shown in Figure 1A, where glucose withdrawal is followed by the gradual failure of the CAP in a representative isolated white matter structure, the P0 RON. The monophasic CAP that is typical at this age[8] shows conduction slowing and CAP decline under 0-glucose conditions. The rate at which glucose withdrawal produced conduction failure was inversely correlated with postnatal age, with significantly different 1/2 time (time taken for a 50% fall in CAP amplitude after the initiation of a challenge) in RONs from P0 to P2 rats compared with those from older animals (Figure 1B). Mean 1/2 time was 28.0 ± 2.6 minutes in P0 to P2 RONs ($n = 13$) compared with 12.2 ± 2.2 minutes in RONs from older animals (P3 tp P14; $n = 8$, $P < 0.001$; Figure 3B).

To examine the importance of metabolic intermediates for maintaining excitability during energy deprivation, glucose and oxygen were withdrawn simultaneously. Compared with the removal of glucose alone, this will block the tricarboxylic acid pathway and leave only glycogen metabolism via glycolysis to support excitability. A similar pattern to that observed during 0-glucose conditions was found under OGD conditions (Figures 2A and 2B), where mean 1/2 time was 32.3 ± 4.2 minutes in P0 to P2 rats ($n = 14$), and 16.1 ± 1.0 minutes in P3 to P17 rats ($n = 13$, $P < 0.001$). The similarity in the rate of CAP decline in the P0 to P2 age range between these two conditions ($P > 0.05$) indicates that tolerance to energy deprivation in early pre-myelinating white matter is independent of the tricarboxylic acid pathway. Glycogen represents the most significant energy reserve in the central nervous system and glycogen utilization can proceed during OGD

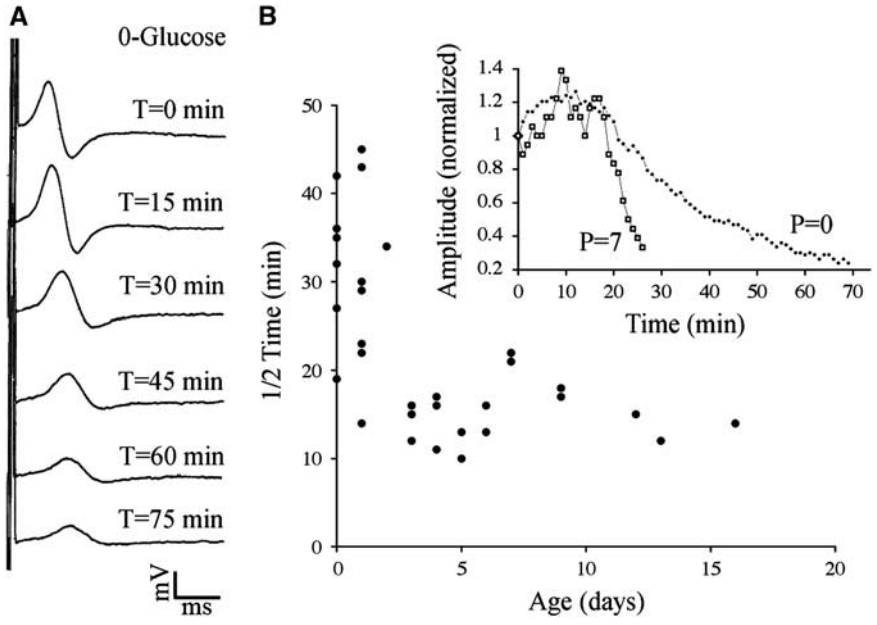

Figure 1. (**A**) Conduction failure during perfusion with 0-glucose in P0 to P2 RON. Compound action potentials recorded from a P0 RON are shown before and after the initiation of perfusion with 0-glucose (the mono-phasic CAP follows the stimulus artifact). Scale = 1 mV/ms in this and all subsequent figures. (**B**) The rate at which the CAP declines during OGD is plotted as the 1/2 time (time to a 50% fall in CAP amplitude) versus postnatal age. Representative data, including that collected from the CAPs in 'B', are shown in the insert. CAP, compound action potential; OGD, oxygen–glucose deprivation; RON, rat optic nerve.

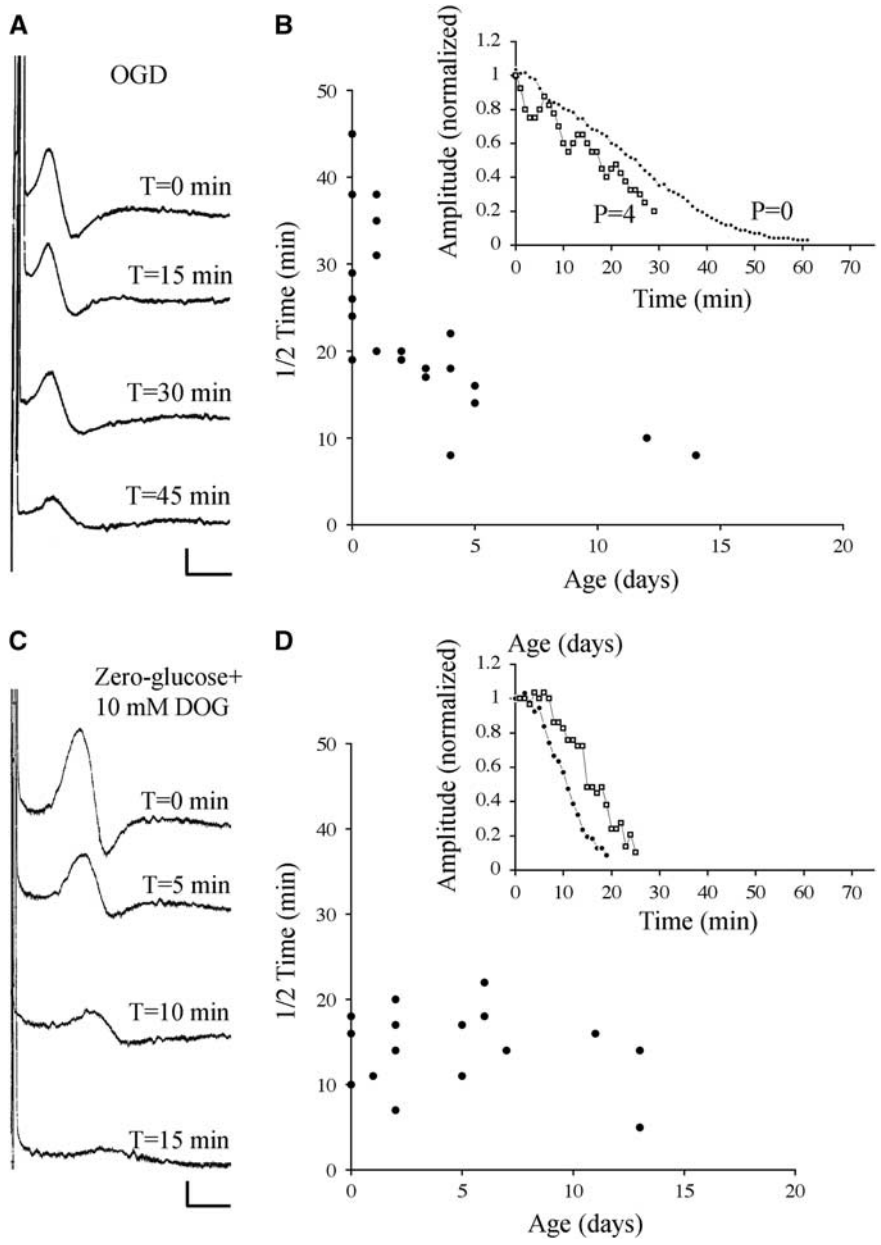

Figure 2. The significance of O_2-dependent and DOG-sensitive energy reserves in P0 to P2 RON. (**A**) Compound action potentials recorded from a P0 RON before and after initiation of OGD. (**B**) 1/2 time for CAPs recorded from RONs at various postnatal ages with representative data shown in the insert. (**C** and **D**) A similar data set showing the effects of glucose withdrawal in the presence of 10 mM DOG. Note that 1/2 times in P0 to P2 RONs are now similar to those recorded from older animals. Scale = 1 mV/1 ms. CAP, compound action potential; DOG, deoxyglucose; OGD, oxygen–glucose deprivation; RON, rat optic nerve.

via glycolysis. Under zero-glucose conditions, astrocytic glycogen degradation is inhibited by the glucose analog 2-deoxyglucose (2-DOG).[12] Perfusion with 0-glucose+10 mM 2-DOG produced rapid conduction failure in P0 RONs (Figure 2C), and the 1/2 time in nerves from P0 to P2 rats (13.8 ± 1.4 minutes, $n = 9$) was not significantly different from that in nerves from P3 to P14 rats (14.6 ± 1.8 minutes, $n = 8$; $P > 0.05$).

The data in Figure 2 suggest that greater access to glycogen underlies the heightened tolerance to energy deprivation in P0 RON. Alternative explanations include a decrease in metabolic rate at this age, or the presence of a cellular factor such as ionotropic glutamate receptor,[13] or calcium channel,[11] expression in RON after P2 that predisposes to rapid conduction failure during energy deprivation. In either case, axons might function for longer at P0 to P2 with a similar glycogen reserve to that present after P2, although neither hypothesis is consistent with the loss of selective 0-glucose tolerance in the presence of 2-DOG. To test these alternative hypotheses, RONs were exposed to combined chemical block of glycolysis (10 mM NaF) and mitochondrial respiration (1 μg/mL antimycin A), which will halt all energy production inside the cell.[14] Under these conditions, cellular energy reserves are inaccessible and differences in cell metabolic rate are removed. Injury mechanisms will therefore be triggered at the same point in white mater at all ages and a high cellular susceptibility to energy deprivation will predispose to a rapid loss-of-function. The effects of metabolic arrest are shown in a repre-

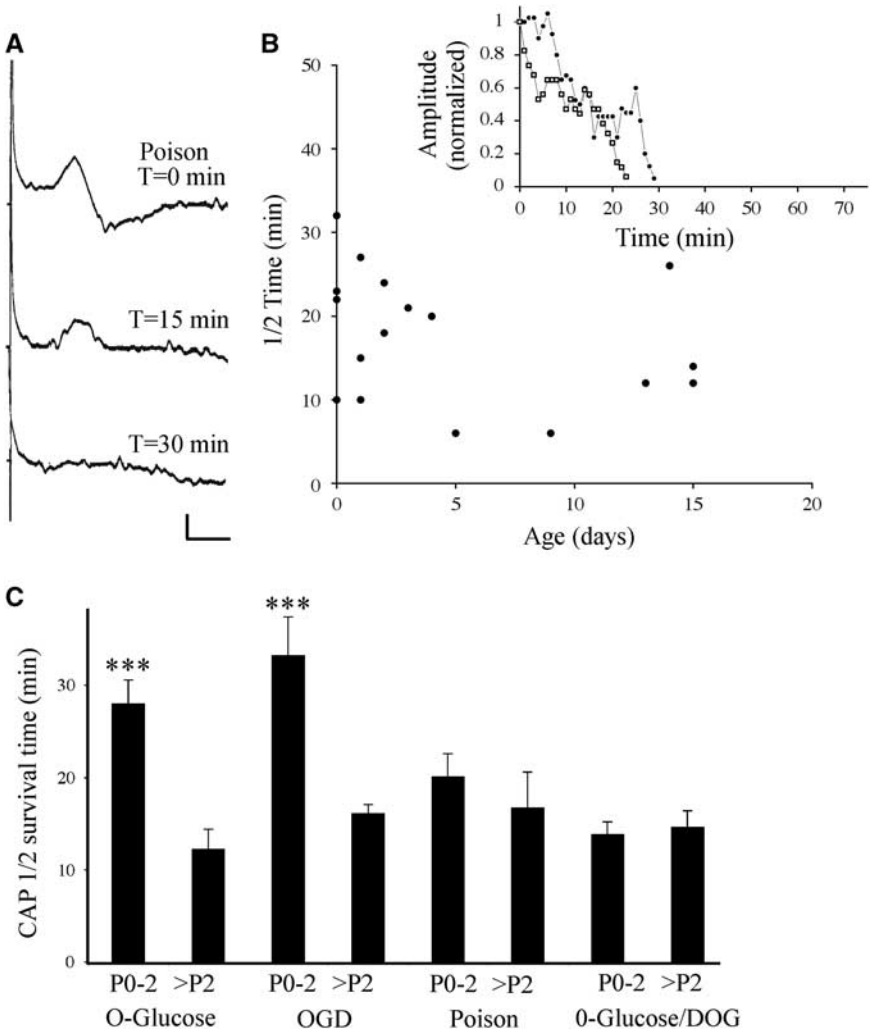

Figure 3. The effects of metabolic arrest on CAP conduction in P0 to P2 RON. (**A**) Compound action potentials recorded from a P0 RON before and after initiation of perfusion with 10 mM NaF+1 μg/mL antimycin A. (**B**) 1/2 time of CAPs recorded from RONs at various postnatal ages with representative data shown in the insert. (**C**) Mean 1/2 time for P0 to P2 and >P2 RONs under the various conditions. Note that the youngest nerves have higher survival times only under conditions where glycogen can be metabolized. Scale = 1 mV/ ms. CAP, compound action potential; RON, rat optic nerve. ***$P < 0.001$ vs. >P2.

sentative P0 RON in Figure 3A and the 1/2 time is plotted against postnatal age in Figure 3B. There is no significant difference in 1/2 time between optic nerves from P0 to P2 rats (20.1 ± 2.5 minutes, $n = 9$) and those from P3 to P15 rats (16.7 ± 3.9 minutes, $n = 7$; $P > 0.05$). The data for all four conditions are pooled in Figure 3C, confirming that significantly longer survival times are found only in P0 RONs during 0-glucose and OGD conditions.

P0 to P10 RONs are not subject to irreversible loss of excitability after 60 minutes of 0-glucose perfusion,[8] and therefore do not suffer permanent injury within this time-frame. To test whether glycogen contributes to this effect, we examined CAP recovery in a 60 minutes 0-glucose+2-DOG perfusion protocol applied over a range of ages. CAPs from P0 to adult RONs suffered a variable degree of irreversible conduction failure after 60 minutes perfusion with 0-glucose+2-DOG (Figure 4). Compound action potentials recovered to 51.2% over the P0 to P10 age range with no significant difference in P0 to P2 nerves (55.3 ± 6.5% CAP recovery, $n = 8$) compared with P3 to P11 (43.7 ± 8, $n = p$; $P > 0.05$). Perfusion with 2-DOG alone had no effects on the CAP at any age (Figure 4C).

The rate of cellular oxidative metabolism is correlated with the proportion of cell volume given over to mitochondria, and mitochondrial volume fraction calculated from ultra-micrographs is used to examine the relative capacity of cellular elements within adult optic nerve to generate ATP (for example, ref. 15). Collages of high-gain ultra-micrographs were constructed from cross-sections of RONs, revealing mitochondrial profiles in axons (for example, Figure 5A 'Mt') and astrocytes (for example, Figure 5B 'Mt') in P0 RON. Mitochondrial volume fraction was calculated from axons at P0 ($n = 404$ axons) and P10, with non-myelinated ($n = 200$) and myelinated ($n = 40$) axons analyzed separately at P10. No significant differences were observed between these axon populations and values were similar to those reported in mature myelinated optic nerve axons (Figure 5C; ref. 15). Astrocytes at P0 ($n = 6$) and P10 ($n = 6$) were also analyzed, revealing values that were not significantly different from those of the surrounding axons (Figure 5C). Immature oligodendrocytes are known to be have an elevated metabolic rate associated with myelin production, and exhibited a mitochondrial volume fraction approximately four times higher than that found in the other cellular elements making up developing white matter (Figure 5C;

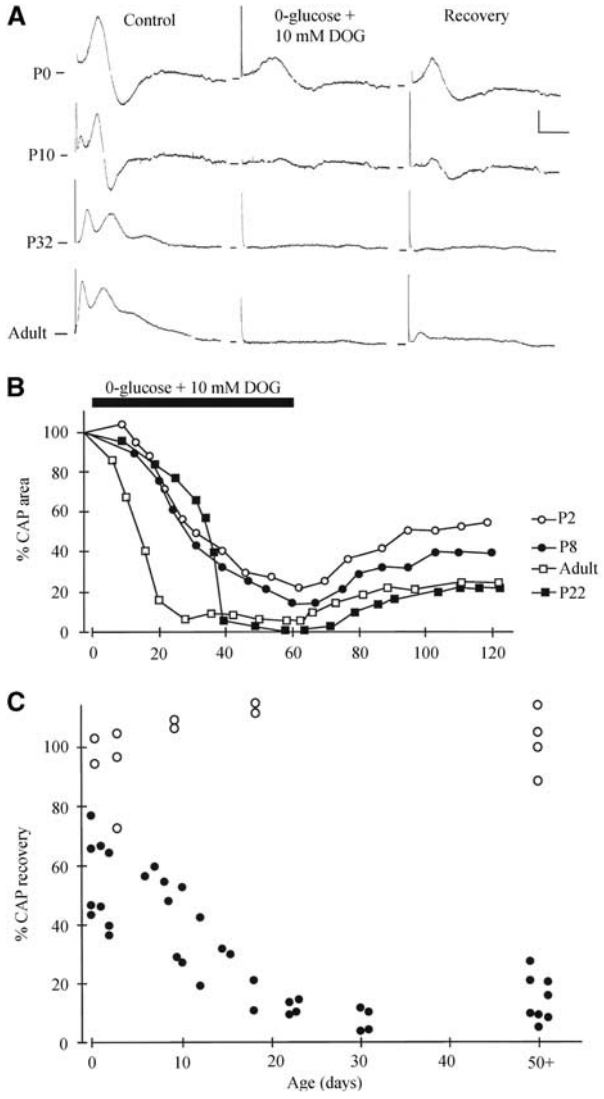

Figure 4. Zero-glucose+10 mM DOG produced irreversible conduction failure. (**A**) Representative CAPs recorded at four different ages are shown before ('control'), 60 minutes after initiation of perfusion with 0-glucose+10 mM DOG, and 60 minutes after reperfusion with aCSF ('Recovery'). (**B**) Plot of representative data showing the date of decline in the CAP under this condition in RONs from animals of different ages. (**C**) CAP recovery after 60 minutes of perfusion with zero-glucose+10 mM DOG (black symbols) plotted against postnatal age. Note the similar level of recovery from P0 to P10. Open symbols show the change CAP recovery after 60 minutes of perfusion with 10 mM DOG alone (glucose present), followed by 60 minutes of recovery in aCSF. aCSF, artificial cerebrospinal fluid; CAP, compound action potential; DOG, deoxyglucose; RON, rat optic nerve.

$n = 6$). The distribution of individual mitochondria in axons in a representative ultra-micrograph collage is shown in Figure 5D by the pink dots.

The data suggest that glycogen is significant for the heightened tolerance to energy deprivation found in pre-myelinated white matter. Prior studies of mature central nervous system report the presence of glycogen alpha particles in astrocytes but not neuronal elements (for example, ref. 16). Ultrathin sections were stained with potassium ferricyanide to enhance glycogen particle contrast and the distribution of particles was examined in high-gain ultra-micrograph collages. Individual alpha particles were found only in astrocytes, as indicated in Figures 5A and 5B, (arrows) and for a single astrocyte in Figure 5D by the green dots (blue dots are glycogen particles present in astrocytes processes that were not contiguous with the soma in this plan of section). While ribosomes were occasionally seen in axon profiles, they were distinguished from glycogen particles by comparison to ribosomes attached to endoplasmic reticulum (Figure 5A 'ER').

A glycogen energy reserve located in astrocytes cannot be directly transmitted to neighboring axons in the absence of oxygen since metabolic intermediates such as lactate require the operation of oxidative phosphorylation to yield ATP. One possible mechanism whereby the astrocytic energy reserve can protect axons in perinatal white matter would involve the maintenance of astrocyte homeostatic functions during energy deprivation, thus protecting near-bye axons. High-power ultra-micrographs of a large section of P0 RON that had been subjected to 90 minutes of OGD+60 minutes recovery were collaged (Figure 6A) to allow the location of healthy axons to be plotted relative to astrocyte somata and processes. In this protocol, the number of identifiable axons that had survived injury was small and there were extensive areas of un-identifiable flocculent debris. The location of all surviving axons, identified by the presence of microtubules and a complete axolemma, are plotted in Figure 6B as green dots. There is a clear injury gradient, with larger number of identifiable axons toward the perimeter of the nerve.

Astrocytes within the nerve section are outlined in various colors in Figure 6A, and the density of axons within a 1-μm zone surrounding these cells is plotted against the depths within the nerve in Figure 6C (black bars). The density of viable axons that are not located in a peri-astrocyte zone is shown in Figure 6C (white bars), revealing higher number of surviving axons immediately around astrocytes at any given depth within the nerve.

DISCUSSION

Developing central white matter is the focus of injury in lesions such as periventricular leukomalacia, which may be the leading correlate of cerebral palsy.[2,3] Such white matter injuries are ischemic in nature and may include focal necrotic lesions or defuse gliotic changes with a peak incidence between PCW 20 and PCW 32. Ischemia-sensitive Pre-Ols populate the white matter structures affected in increasing numbers from PCW 28, but are present at low densities prior to PCW 28 and the exact timing and focus of proliferation may vary between cortical regions.[2,17] The co-incidence of the maturation of the oligodendrocyte lineage into the pre-Ol stage with predilection to injury suggests that selective damage to these cells is the key neuropathological event.

Mature-phenotype, GFAP(+) astrocytes are present in the human fetal brain from ~PCW 11 to PCW 14,[18] and populate the intermediate zone from PCW 16 to PCW 18.[4] Fibrous white matter astrocytes appear before protoplasmic gray matter astrocytes, and the subsequent expansion of cortical white matter markedly increases the spacing between astrocyte somata.[4,5] When radial glia are taken into consideration, the fall in support glia (radial glia+astrocyte) density in maturing white matter is dramatic.[19,20] Studies of glial cell density in central white matter can be confounded by the complex morphological arrangement of tracts containing axons of different diameters and maturational stage. Large differences in astrocyte development have been noted, for example, between closely apposed fiber tracts in the optic radiations.[4] These complications are avoided in the optic nerve, which is a uniform and structurally isolated white matter tract where astrocytes are generated from astrocyte precursor cells rather than by transformation of radial glia.[21] By mid-gestation, human optic nerve astrocyte maturation is largely complete, predating the onset of myelination by ~20 weeks.[16] In rodent studies, astrocyte precursor cell populate the RON at fetal day 17, and GFAP(+) astrocytes are generated continually until the first days of life.[6,7,21] Numerous reports find a RON astrocyte

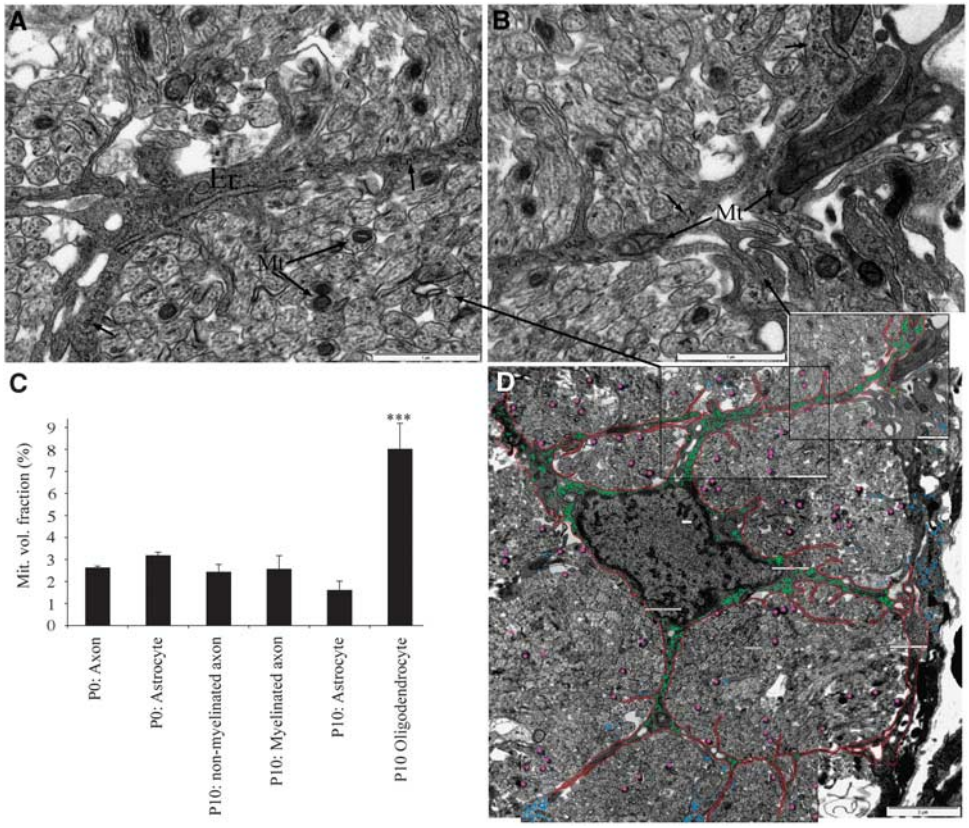

Figure 5. Glycogen and mitochondria in P0 RON. (**A** and **B**) Higher power electron micrographs of P0 RON in cross-section, showing an astrocyte process containing endoplasmic reticulum ('ER'), mitochondria ('Mt') and glycogen particles (arrows). Mitochondria are also found in axon profiles (**A**). (**C**) The mitochondrial volume fraction in axons, astrocytes, and oligodendroglia in P0 and P10 RON. Note that only oligodendroglial cells in P10 RON have an elevated mitochondrial volume fraction and that P0 axons have a similar mitochondrial volume fraction to other cellular elements ("***" $P < 0.001$ versus all other means). (**D**) Low power electron micrograph collage showing the location of all glycogen particles (which were only found in the astrocyte soma and processes; green dots) and mitochondria (only axonal mitochondria are shown; pink dots). Blue dots represent glycogen particles within astrocyte processes that could not be traced back to the main cell in the center of the section. The location of **A** and **B** are also indicated. Scale = 1 μm (**A** and **B**) and 2 μm (**C**). RON, rat optic nerve.

population of 70 to 120 cells/cross-section from P0-adult and astrocyte density and relative volume therefore fall as the nerve diameter increases in the perinatal period.[6,22–25] A similar phenomena has been reported for numerous white matter tracts in mouse, where GFAP content is maximal immediately before the start of the myelination program and declines thereafter.[26]

The current experiments suggest that a fall in astrocyte density as white matter prepares for the onset of myelination underlies a rise in sensitivity to ischemic injury. The high ischemic tolerance of very immature white matter has been observed previously,[8] and has generally been ascribed to a putative low metabolic rate before the arrival of pre-OIs in the RON. However, analysis of mitochondrial volume fraction found no significant difference in energy capacity between P0 and P10 in axons or astrocytes, although P10 oligodendroglia had a higher energy capacity consistent with a high metabolic rate in these cells. In fact, the energy capacity of axons calculated in this way was similar to that reported for mature RON axons,[15] indicating that similar metabolic demands are placed on immature and mature axons. This surprising finding is consistent with reports showing that glucose utilization rate, blood flow, and vascularization reach near-adult levels in central white matter early in development,[27,28] including in humans (for example, ref. 29).

Neonatal and mature retinal ganglion cells fire action potentials with a similar mean frequency (~10 Hz).[30] The axons of the neonatal ganglion cells transmit long-duration action potentials down the optic nerve[31] which will require high levels of axonal Na-K ATPase activity to maintain ionic gradients. Saxitoxin-binding studies suggest low levels of voltage-gated Na^+ channel expression in perinatal RON axons,[32] but we have recently shown that voltage-gated Ca^{2+}-channels contribute significantly to the action potential in pre-myelinated axons,[11] and freeze-fracture studies find no significant differences in membrane particle density in RON axons over the first several weeks of life.[33] The area of active membrane mediating an action potential is far greater in a pre-myelinated axon than in a myelinated axon, and metabolic demand is approximately threefold higher in mature RON axons at their non-myelinated retinal segments than at their myelinated nerve segments.[34] Perinatal RON axons are also undergoing a rapid growth in axolemma volume because of radial expansion, and are heavily loaded with vesicular and tubular elements requiring axoplasmic transport.[11,35] These considerations are consistent with a relatively high energy capacity in pre-myelinated central axons.

If a low metabolic rate does not account for the high ischemic tolerance of early pre-myelinated white matter, it may be that the cellular mechanisms of injury are different at this point in development. In mature RON axons, ischemic conditions lead to acute injury after influx of Na^+ and Ca^{2+} through voltage-gated Ca^{2+} and Na^+ channels coupled to reverse Na-Ca exchange. [1] Ion

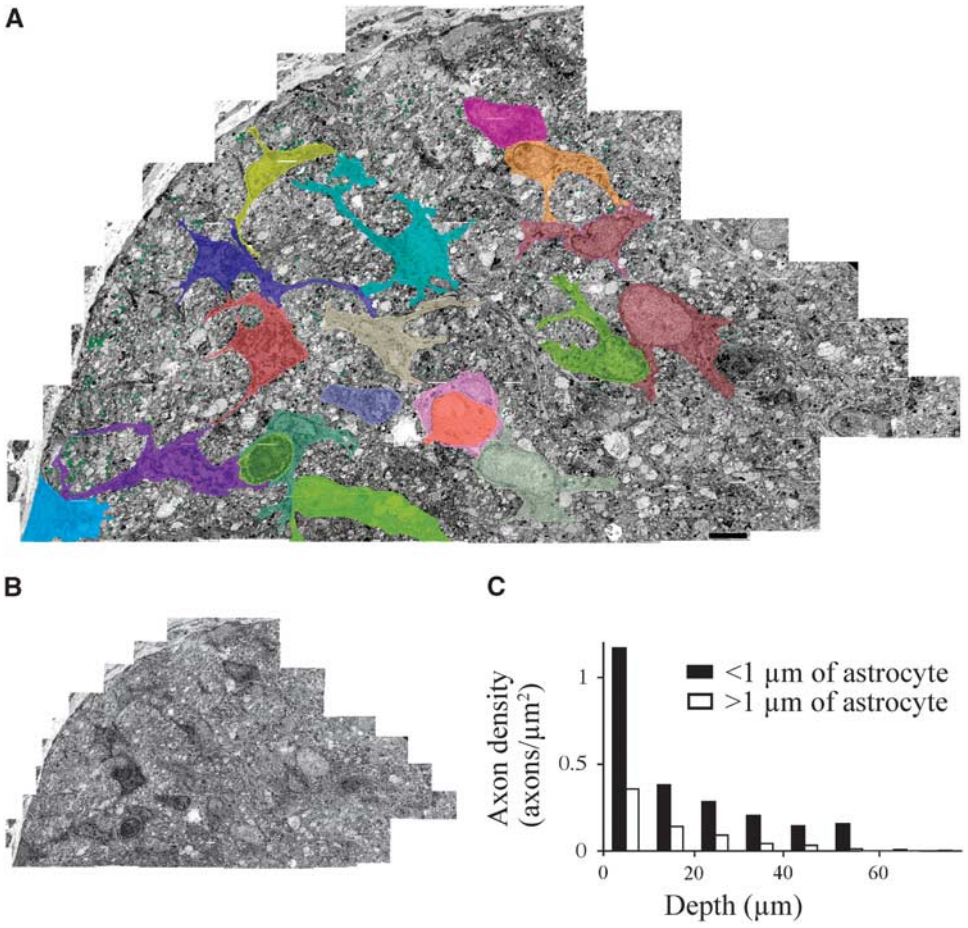

Figure 6. Axon injury distribution in P0 RON subjected to 90 minutes of OGD+60 minutes of recovery. (**A**) Low power electron micrograph collage cross-section of P0 RON after 90 minutes of OGD+60 minutes recovery. The distribution of all viable axons (green dots) and the morphology of all astrocytes (colored) are shown. Scale = 4 μm. (**B**) The same section, shown without markings. (**C**) Axon density plotted as a function of depth from the surface for axons located within 1 μm of an astrocyte (filled bars) or outside these zones (open bars). Note that there is a higher density of viable axons in the immediate environment of an astrocyte. OGD, oxygen–glucose deprivation; RON, rat optic nerve.

channel expression patterns evolve dramatically during postnatal axon development, but not within the first few days of life,[11,36] while changes in Na–Ca exchange expression have not been examined in developing white matter. Astrocytes in P0 to P4 RON have significantly higher tolerance of ischemia than at P10 because of low levels of Na–Cl–K cotransport expression, which is associated with cytotoxic cell swelling at later periods.[37–39] Such changes in expression of proteins central to white matter injury must have profound consequences for ischemic tolerance; indeed, there are large differences in the degree of injury incurred during energy deprivation in white matter over the postnatal period (Figure 4; ref. 8). However, these events do not appear to underlie the particular ischemic tolerance of early pre-myelinated white matter. Indeed, small pre-myelinated axons indistinguishable from those in P0 RON do not exhibit a high ischemic tolerance in P10 RON.[13]

When all metabolic activity was halted in P0 to P2 RON in the current study, elevated ischemia tolerance was lost. If these perinatal nerves were innately resistant to injury, metabolic stasis would be selectively less effective than in older nerves. Indeed, block of glycogenolysis was sufficient to remove ischemia tolerance indicating that it solely was because of an intracellular glycogen reserve. Consistent with studies on human fetal optic nerve,[16] we found no evidence for the presence of glycogen in developing axons themselves. Robust glycogen deposits were present in astrocytes throughout the postnatal period and it appears that this energy reserve is responsible for the elevated ischemia tolerance of early pre-myelinated central white matter. The relative sparing of axons after prolonged ischemia in zones neighboring astrocyte somata that were rich in glycogen deposits is consistent with this hypothesis.

Astrocytes regulate the extracellular environment within which axons function, including regulation of extracellular glutamate. Glutamate transporter expression is particularly high in P2 RON[40] while glutamate receptor activation is central to injury of developing white matter including axons.[13] The mechanisms of axonal injury in ischemic early pre-myelinated white matter have recently been shown to be mediated by glutamate receptors[41] and we can speculate that improved homeostatic regulation of excitotoxins such as glutamate because of a high density of glycogen-rich astrocytes may contribute to ischemia tolerance. The phenomena has considerable clinical relevance, since the first weeks of the PCW 20 to PCW 32 window of peak incidence for PVL predates the proliferation of pre-OLs and corresponds to the period of transition from early pre-myelinated white matter of high ischemia tolerances to late pre-myelinated white matter with heightened ischemic sensitivity. A similar process may contribute to neurodegenerative diseases of the aging brain. While detecting age-related changes in astrocyte number in humans is technically difficult because of reactive

changes in the cells, there is evidence suggesting a decrease.[42] Glial mitochondrial metabolism is also depressed with aging in humans,[43] and taken together these observation are consistent with reduced astrocyte support of neurons in the aging brain that may predispose it to injury after vascular failure or hypoperfusion.

DISCLOSURE/CONFLICT OF INTEREST

The author declares no conflict of interest.

REFERENCES

1 Fern RF, Matute C, Stys PK. White matter injury: Ischemic and nonischemic. *Glia* 2014; **62**: 1780–1789.
2 Back SA, Luo NL, Borenstein NS, Levine JM, Volpe JJ, Kinney HC. Late oligodendrocyte progenitors coincide with the developmental window of vulnerability for human perinatal white matter injury. *J Neurosci* 2001; **21**: 1302–1312.
3 Khwaja O, Volpe JJ. Pathogenesis of cerebral white matter injury of prematurity. *Arch Dis Child Fetal Neonatal Ed* 2008; **93**: F153–F161.
4 Roessmann U, Gambetti P. Astrocytes in the developing human brain. An immunohistochemical study. *Acta Neuropathol* 1986; **70**: 308–313.
5 Takashima S, Becker LE. Developmental changes of glial fibrillary acidic protein in cerebral white matter. *Arch Neurol* 1983; **40**: 14–18.
6 Vaughn JE. An electron microscopic analysis of gliogenesis in rat optic nerves. *Z Zellforsch Mikrosk Anat* 1969; **94**: 293–324.
7 Skoff RP, Price DL, Stocks A. Electron microscopic autoradiographic studies of gliogenesis in rat optic nerve. II. Time of origin. *J Comp Neurol* 1976; **169**: 313–334.
8 Fern R, Davis P, Waxman SG, Ransom BR. Axon conduction and survival in CNS white matter during energy deprivation: a developmental study. *J Neurophysiol* 1998; **79**: 95–105.
9 Cataldo AM, Broadwell RD. Cytochemical identification of cerebral glycogen and glucose-6-phosphatase activity under normal and experimental conditions. II. Choroid plexus and ependymal epithelia, endothelia and pericytes. *J Neurocytol* 1986; **15**: 511–524.
10 Wender R, Brown AM, Fern R, Swanson RA, Farrell K, Ransom BR. Astrocytic glycogen influences axon function and survival during glucose deprivation in central white matter. *J Neurosci* 2000; **20**: 6804–6810.
11 Alix JJ, Dolphin AC, Fern R. Vesicular apparatus, including functional calcium channels, are present in developing rodent optic nerve axons and are required for normal node of Ranvier formation. *J Physiol* 2008; **586**: 4069–4089.
12 Dringen R, Hamprecht B. Inhibition by 2-deoxyglucose and 1,5-gluconolactone of glycogen mobilization in astroglia-rich primary cultures. *J Neurochem* 1993; **60**: 1498–1504.
13 Alix JJ, Fern R. Glutamate receptor-mediated ischemic injury of premyelinated central axons. *Ann Neurol* 2009; **66**: 682–693.
14 Swanson RA. Astrocyte glutamate uptake during chemical hypoxia *in vitro*. *Neurosci Lett* 1992; **147**: 143–146.
15 Perge JA, Niven JE, Mugnaini E, Balasubramanian V, Sterling P. Why do axons differ in caliber? *J Neurosci* 2012; **32**: 626–638.
16 Sturrock RR. A light and electron microscopic study of proliferation and maturation of fibrous astrocytes in the optic nerve of the human embryo. *J Anat* 1975; **119**: 223–234.
17 Jakovcevski I, Filipovic R, Mo Z, Rakic S, Zecevic N. Oligodendrocyte development and the onset of myelination in the human fetal brain. *Front Neuroanat* 2009; **3**: 5.
18 Wierzba-Bobrowicz T, Lechowicz W, Kosno-Kruszewska E. A morphometric evaluation of morphological types of microglia and astroglia in human fetal mesencephalon. *Folia Neuropathol* 1997; **35**: 29–35.
19 Spreafico R, Arcelli P, Frassoni C, Canetti P, Giaccone G, Rizzuti T *et al.* Development of layer I of the human cerebral cortex after midgestation: architectonic findings, immunocytochemical identification of neurons and glia, and in situ labeling of apoptotic cells. *J Comp Neurol* 1999; **410**: 126–142.
20 Howard BM, Zhicheng M, Filipovic R, Moore AR, Antic SD, Zecevic N. Radial glia cells in the developing human brain. *Neuroscientist* 2008; **14**: 459–473.
21 Mi H, Barres BA. Purification and characterization of astrocyte precursor cells in the developing rat optic nerve. *J Neurosci* 1999; **19**: 1049–1061.
22 Matheson DF. Some quantitative aspects of myelination of the optic nerve in rat. *Brain Res* 1970; **24**: 257–269.
23 Black JA, Waxman SG, Ransom BR, Feliciano MD. A quantitative study of developing axons and glia following altered gliogenesis in rat optic nerve. *Brain Res* 1986; **380**: 122–135.
24 Zhang MZ, McKanna JA. Gliogenesis in postnatal rat optic nerve: LC1+microglia and S100-beta+astrocytes. *Brain Res Dev Brain Res* 1997; **101**: 27–36.
25 David S, Miller RH, Patel R, Raff MC. Effects of neonatal transection on glial cell development in the rat optic nerve: evidence that the oligodendrocyte-type 2 astrocyte cell lineage depends on axons for its survival. *J Neurocytol* 1984; **13**: 961–974.
26 Jacque C, Lachapelle F, Collier P, Raoul M, Baumann N. Accumulation of GFA, the monomeric precursor of the gliofilaments, during development in normal mice and dysmyelinating mutants. *J Neurosci Res* 1980; **5**: 379–385.
27 Nehlig A, Pereira de Vasconcelos A, Boyet S. Postnatal changes in local cerebral blood flow measured by the quantitative autoradiographic [14C]iodoantipyrine technique in freely moving rats. *J Cereb Blood Flow Metab* 1989; **9**: 579–588.
28 Chugani HT, Hovda DA, Villablanca JR, Phelps ME, Xu WF. Metabolic maturation of the brain: a study of local cerebral glucose utilization in the developing cat. *J Cereb Blood Flow Metab* 1991; **11**: 35–47.
29 Orgul S, Cioffi GA. Embryology, anatomy, and histology of the optic nerve vasculature. *J Glaucoma* 1996; **5**: 285–294.
30 Blankenship AG, Hamby AM, Firl A, Vyas S, Maxeiner S, Willecke K *et al.* The role of neuronal connexins 36 and 45 in shaping spontaneous firing patterns in the developing retina. *J Neurosci* 2011; **31**: 9998–10008.
31 Foster RE, Connors BW, Waxman SG. Rat optic nerve: electrophysiological, pharmacological and anatomical studies during development. *Brain Res* 1982; **255**: 371–386.
32 Waxman SG, Black JA, Kocsis JD, Ritchie JM. Low density of sodium channels supports action potential conduction in axons of neonatal rat optic nerve. *Proc Natl Acad Sci USA* 1989; **86**: 1406–1410.
33 Black JA, Foster RE, Waxman SG. Rat optic nerve: freeze-fracture studies during development of myelinated axons. *Brain Res* 1982; **250**: 1–20.
34 Perge JA, Koch K, Miller R, Sterling P, Balasubramanian V. How the optic nerve allocates space, energy capacity, and information. *J Neurosci* 2009; **29**: 7917–7928.
35 Hildebrand C, Waxman SG. Postnatal differentiation of rat optic nerve fibers: electron microscopic observations on the development of nodes of Ranvier and axoglial relations. *J Comp Neurol* 1984; **224**: 25–37.
36 Rasband MN, Shrager P. Ion channel sequestration in central nervous system axons. *J Physiol* 2000; **525**: 63–73.
37 Fern R. Intracellular calcium and cell death during ischemia in neonatal rat white matter astrocytes in situ. *J Neurosci* 1998; **18**: 7232–7243.
38 Thomas R, Salter MG, Wilke S, Husen A, Allcock N, Nivison M *et al.* Acute ischemic injury of astrocytes is mediated by Na-K-Cl cotransport and not Ca2+ influx at a key point in white matter development. *J Neuropathol Exp Neurol* 2004; **63**: 856–871.
39 Salter MG, Fern R. The mechanisms of acute ischemic injury in the cell processes of developing white matter astrocytes. *J Cereb Blood Flow Metab* 2008; **28**: 588–601.
40 Choi I, Chiu SY. Expression of high-affinity neuronal and glial glutamate transporters in the rat optic nerve. *Glia* 1997; **20**: 184–192.
41 Huria R, Murthy B, Al-Ghamdi B, Fern R. Pre-myelinated central axons express neurotoxic NMDA-receptors: relevance to white matter injury. *J Cereb Blood Flow Metab* 2015. doi10.1038/jcbfm.2014.227.
42 Mansour H, Chamberlain CG, Weible MW, 2nd, Hughes S, Chu Y, Chan-Ling T. Aging-related changes in astrocytes in the rat retina: imbalance between cell proliferation and cell death reduces astrocyte availability. *Aging Cell* 2008; **7**: 526–540.
43 Boumezbeur F, Mason GF, de Graaf RA, Behar KL, Cline GW, Shulman GI *et al.* Altered brain mitochondrial metabolism in healthy aging as assessed by in vivo magnetic resonance spectroscopy. *J Cereb Blood Flow Metab* 2010; **30**: 211–221.